INTERNATIONAL JOURNAL OF HEAT AND TECHNOLOGY

ISSN: 0392-8764
Vol. 35, No. 1, March 2017, pp. 153-166
DOI: 10.18280/ijht.350121

A publication of IIETA

IIETA International Information and Engineering Technology Association
Advancing the World of Information and Engineering
http://www.iieta.org/Journals/IJHT

# Flow and thermal characteristics of jet impingement: comprehensive review

Anuj K. Shukla, Anupam Dewan *

Indian Institute of Technology Delhi, Hauz Khas, New Delhi - 110016, India

Email: adewan@am.iitd.ac.in

## ABSTRACT

A comprehensive review on jet impingement heat transfer is presented to consider the state-of the art in this field. Among all the single-phase heat transfer arrangements possible, it has the maximum heat transfer rate. A number of arrangements are possible to represent a practical or physical situation, such as, jet impingement on a solid flat surface or surface fitted with different kinds of turbulent promoters, inclined plane surface and cylindrical convex/concave surface, etc. A significant number of papers dealing with experimental and computational studies on different physical and computational aspects of jet impinging flows are reviewed. Several parameters were found to influence the characteristics, such as, flow confinement, nozzle shape, jet to plate spacing and Reynolds number. An extremely small number of studies dealing with application based jet impingement heat transfer configurations (e.g., ribs fitted impingement plate, moving impingement plate, etc) experimentally and numerically have been reported in the literature. Various computational approaches, such as, RANS, LES, DNS and hybrid models, that are used to study the jet impingement heat transfer, with their complexities and boundary conditions, have been reviewed. It was observed that majority of RANS based turbulence models did not predict impinging flows accurately and its complexities except a few. Many authors have reported that LES is capable of predicting the flow field and heat transfer data within the accepted accuracy limits. DNS can be applied to simple geometry with low Reynolds number. Recently some authors have employed hybrid models, such as, PANS, DES, etc., and concluded that these models provide reasonably accurate results and were found to be computationally less expensive than LES and DNS.

**Keywords:** Jet Impingement, Ribs, Turbulence, Nusselt Number, LES.

## 1. INTRODUCTION

Jet impingement heat transfer is an interesting flow configuration to study because of its industrial as well as fundamental significance. Among all the single-phase heat transfer arrangements, it has the maximum heat transfer rate [1]. Due to growing demand of heat transfer enhancement in many industrial applications, jet impingements are widely used and studied. These techniques are used wherever high performance cooling, heating or drying of a surface is required. Some important industrial applications are cooling/heating of electrical equipment, drying requirements associated with textile and paper industries, cooling of turbine blades and outer combustor wall, freezing of tissues in cryosurgery, annealing of glass, rapid cooling or heating involved in glass manufacturing and short-take-off/vertical landing (STOVL) aircrafts, etc. Impinging jets offer an effective and flexible approach to transfer energy or mass in many industrial applications by changing the flow and geometric parameters, such as, jet Reynolds number (*Re*), nozzle geometry/shape, assembly of jet array, nozzle-to-plate spacing, angle of jet impingement, turbulence properties at the exit of the jet, ribbed surfaces and flow pulsation, etc.

Although jet impingement on a plate is geometrically simple, it involves a number of interesting complex physical flow configurations, namely, free-shear region (realization of large scale vortex structures), stagnation region (with strong streamline curvature) and a wall jet region. With escalating requirements for industrial efficiency and safety, slot and round jet impingements on a plane surface have been studied by the researchers. Several arrangements are possible to represent a physical situation involving, such as, jet impingement on a solid flat surface or surface fitted with different kinds of turbulent promoters, inclined plane surface and cylindrical convex/concave surface, etc. In the present paper we have considered a number of experimental and computational approaches used in the literature for jet impingement heat transfer to assess the state-of-the art in the field.

### 1.1 Flow patterns

A flow with air jet impingement orthogonally on a flat surface follows some distinct regions (Fig. 1). At the nozzle exit, the emerging jet may pass through a region where it is sufficiently far-off from the impingement plate so that it acts like a free submerged jet or free jet region. In this region, the

entrainment of mass, momentum and energy occurs due to shear-driven interaction of the surroundings with existing jet. The fluid from the surroundings gets entrained in to the jet and hence there is a reduction in the jet velocity with an increase in the total mass flow rate. In the process, the jet loses kinetic energy and the velocity profile expands in the spatial direction and shrinks down in magnitude along the sides of the jet. Thus, a non-uniform radial velocity profile develops within the jet. Further the free jet can be sub-divided into three regions, namely, the potential core, developing and developed regions.

The shear-layer or mixing-layer surrounds a core where the nozzle centerline fluid velocity ($U_m$) is approximately equal to the jet exit velocity and this region is called the potential core. The end of a core region may be defined as the point where $U_m = 0.95U_{exit}$ [2]. The length of the potential core significantly depends on the jet exit flow conditions and geometry of the nozzle. The length of the potential core zone is found to be nearly 6-7 diameters and 4.7 - 7.7 slot widths from the nozzle exit for round and slot jets, respectively [2]. After the potential core, the axial velocity profile decays due to large shear stresses at the boundary of the jet and this region is characterized as the developing zone. After the developing zone, a fully developed velocity profile is obtained and it is designated as the developed region (Fig. 1).

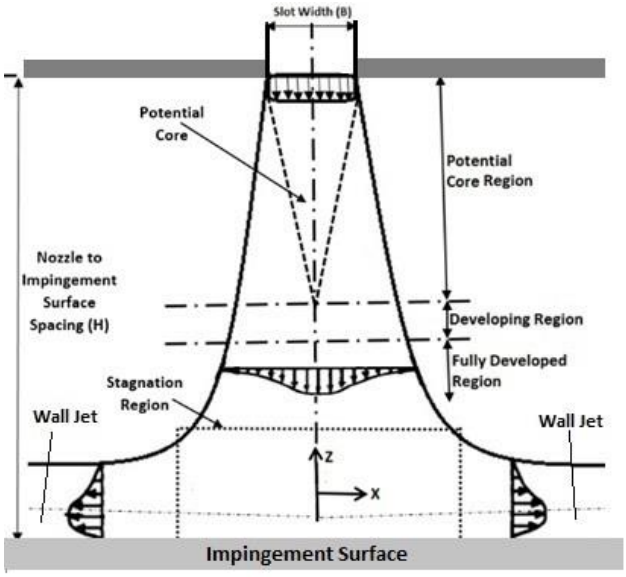


**Figure 1**. Different regions of a jet impingement flow

A free jet region may not be present if the nozzle exit lies at a distance of two diameters or slot widths from the target plate [3]. Schlichting [4] showed that the jet half width (a distance where $U = U_m/2$ down the jet axis) and reduction in the center line velocity are directly related to the axial distance after the termination of the potential core. At the point where the jet strikes, the impingement surface is often referred to as the deflection zone/ stagnation region. In this region, the axial velocity quickly diminishes with a consequent rise in the static pressure. Thereafter the wall jet region, where the bulk flow is in the radial outward direction, becomes important (Fig. 1).

A comprehensive review of the relevant literature is presented here. It consists of different physical and computational aspects of impinging flows. Most reported studies have presented profiles of mean velocity, turbulence and heat transfer rates in different regions of the impinging flow. Heat transfer is generally expressed in terms of Nusselt number ($Nu$), defined as $hB/k$, with $h$, $B$ and $k$ representing heat transfer coefficient at the surface, hydraulic diameter (slot width, $B$ in case of slot jets) of the nozzle and thermal conductivity of the plate material, respectively. It was observed that the stagnation point Nusselt number ($Nu_{st}$) and the surface distribution of $Nu$ are the most widely reported quantities in the literature. All these quantities depend on some basic parameters discussed here.

## 2. EXPERIMENTAL STUDIES ON IMPINGING FLOWS

Jet impingement heat transfer and flow features depend on various parameters, namely, jet $Re$, Prandtl number ($Pr$), heat transfer coefficient ($h$), turbulence at the jet exit, nozzle geometry, flow confinement, spacing between jet exit to impingement plate ($H/B$) and distance from the stagnation point ($x/B$), etc. The effect of these parameters on flow field and heat transfer characteristics of slot jet impingement has found special attention in the literature both experimentally and computationally [3, 5-7].

Gardon *et al.* [8] showed that in case of impinging jets, the heat transfer properties cannot be understood with velocity and position dependent boundary-layer thickness only. These can, however, be explained by considering the influence of turbulence. Koopman and Sparrow [9] experimentally studied the effect of a row of impinging jets on plane surface on the local and average heat transfer coefficients. They showed relatively high local heat transfer coefficient in the mid-way between the neighboring jets due to the collision of the spreading flows from nearby jets. They also showed that at the stagnation point the maximum heat transfer occurs and it depends upon the jet to plate distance. Baines and Keffer [10] observed the shear stress to be minimum at the stagnation point with a local maxima in nearby regions. The effect of small nozzle to plate spacing on $Nu_{st}$ and $Nu$ was investigated by many researchers, such as, Hoogendoorn [5], Lytle and Webb [11], and Ashforth-Frost *et al.* [3].

Hoogendoorn [5] observed that the Nusselt numbers were slightly higher in the vicinity of the stagnation point than at the stagnation point for $z/D < 5$ and $Re = 20000$ to 90000. Lytle and Webb [11] experimentally investigated jet impingement heat transfer for the nozzle to plate spacing of less than one diameter. They considered nine values of $Re$ from 3600 to 27600 and observed considerable augmentation in mean velocity and r.m.s. turbulence fluctuations with a reduction in the nozzle to plate spacing. They showed significant enhancements in heat transfer and turbulence level due to forced acceleration of impinging fluid for small spacing. Asforth-Frost and Jambunathan [6] studied the effect of semi-confinement and nozzle geometry for axisymmetric air jet on the potential core at a $Re$ of 22500. They showed that the potential core was 7% longer for fully developed condition compared to the flat jet exit condition. They also observed extended potential core by up to 20% for a semi-confinement case compared to an unconfined case, and reduced stagnation point heat transfer by 10%. The maximum stagnation point heat transfer was obtained when the impingement plate was placed at the end of the potential core. Tu and Wood [12] experimentally measured wall pressure and shear stress for 2-D turbulent jet impingement on a flat plate. The uncertainties associated with the pressure

measurement were ±2% and ±5% for the wall shear stress measurement, respectively. They performed experiments with *Re* from 3040 to 11000 and several *H/D* values and observed a Gaussian distribution of the mean static pressure independent of *Re*. The shape of the wall shear stress distribution depended on both *Re* and the nozzle to plate spacing. They showed that the half width (*b*) of the pressure profile increased with plate spacing. Their data may be used to validate numerical models.

Ashforth-Frost *et al.* [3] experimentally investigated velocity and turbulence characteristics of a semi-confined impinging slot jet. They considered *H/B* of 4 and 9.2 with *Re* = 20000 and showed that the length of the potential core was longer with the semi-confined arrangement than with the unconfined arrangement due to narrow entrainment and scattering of jets. For the impinging jet, turbulence characteristics and velocity were found directly in relation to heat transfer. They also observed that for a low nozzle to plate spacing a secondary peak in *Nu* was distinct. Maurel and Solliec [13] experimentally investigated the development of the jet impinging normally on a flat plate using LDV and PIV with variable geometry. They considered turbulence intensity at the nozzle exit between 1.6% to 2.8% and *Re* from 67000 to 110000. From their parametric study they concluded that the characteristic height of the impinging zone was close to 12-13% of the total height (*H*). Zhe and Modi [7] experimentally studied velocity field near the target surface for a 2-D slot jet impingement configuration with *H/B* from 2 – 9.2 and jet *Re* from 10000 – 30000. They employed a boundary-layer probe at a distance of approximately $y^+ = 2$ to 4 in order to document the wall shear stress. The length in the *z*-direction was considered six times of its slot width. The uncertainties in their near wall measurement were 9% and mean and root mean square velocity were 4% and 3%, respectively. They carried out all the measurements in the region of $x/B = \pm 13$ and $y/B = 0$ to 0.35 at $z = 0$ plane. They observed that the skin friction coefficient was independent of *Re* in the range of 10000 to 20000 and on the other hand it was observed to depend on *H/B* value. However at *H/B* = 2, 3 and 4 it showed slight variations. The shear at low nozzle to plate spacing showed a clear secondary peak which was absent at higher nozzle to plate spacing. Their experimental data may be used to validate numerical models.

O'Donovan and Murray [14] experimentally investigated flow field and heat transfer characteristics from a heated flat plate with *H/B* of 0.5 to 8 and *Re* from 10000 to 30000. They showed secondary peaks in heat transfer distributions in the radial direction for jet to plate spacing less than two diameters owing to a sudden growth in turbulence in the wall jet region. They also showed that high heat transfer regions are associated with the high fluid velocity and turbulence intensity regions. They observed peaks in heat transfer distribution at locations where the velocity fluctuations in normal direction to impingement plate were high. Further O'Donovan and Murray [15] experimentally investigated the temporal nature

of heat transfer and fluid flow with the values of all parameters being same as in their former study. They showed that the growth of vortices through the distance from the jet axis affected the heat transfer coefficient in the wall jet region.

Alekseenko *et al.* [16] experimentally studied the influence of swirl rate of an impinging jet on flow field using PIV and stereo PIV techniques. They considered *H/D* = 3, *Re* = 8900 and swirl rate from 0 - 1.0 and observed a decreased level of pressure diffusion with increasing swirl rates. They showed a large recirculation zone between the jet exit and the impinging surface at a swirl rate of 0.41 and vortex breakdown at swirl rates of 0.70 and 1.0 with a smaller recirculation. Strong generation of turbulence was observed due to vortex breakdown resulting in high values of *TKE* in the local regions. Bakirci and Bilen [17] experimentally visualized the temperature distribution on the impingement surface maintained at a constant temperature for the multi-channel, swirling and conventional jet impingements by means of liquid crystal technique. They used swirl generator insert with the swirl angle fixed at $0^0$, $22.5^0$, $41^0$ and $50^0$ to alter the direction and strength of the swirl. The local Nusselt numbers for the multi-channel impinging jet (at an angle of $0^0$) were found much higher than those for other two configurations. The positions of the heat transfer peaks were moved sensitively from the stagnation point, when swirl angles were increased but decreased values of local and average Nusselt numbers were observed when swirl angles were increased.

Senter and Solliec [18] experimentally investigated flow field of a confined turbulent slot jet impinging orthogonally on a moving flat surface using PIV. They performed experiments for *H/B* = 8, *Re* = 5300, 8000 and 10600 and four surface to jet velocity ratios (0, 0.25, 0.5 and 1). They observed that the flow field topology was independent of *Re* ranging from 5300-10600 at a particular surface to jet velocity ratio. They observed a slightly affected flow field at a surface to jet velocity ratio of 0.25 and the most influenced flow field pattern was found at the surface to jet velocity ratio of unity. Turbulence intensity measurements in the vicinity of the stagnation zone showed enhanced values with increasing surface to jet velocity ratio.

Ozmen [19] experimentally analyzed flow characteristics of confined twin air jets impinging normally on a surface at high *Re* with the smoke wire technique. The uncertainties associated with axial velocity and turbulence velocity measurements in the vertical direction were ±3% and ±4%, respectively, and with pressure measurement it was ±2%. He obtained pressure distribution on the impingement and confined surfaces with *Re* in the range of 30000 to 50000, *H/D* 0.5 to 4 and jet to jet spacing (*L/D*) 0.5 to 2. He observed sub-atmospheric region at the nozzle to plate spacing up to 1 diameter on impingement and confined plate both for the range of *Re* and jet to jet spacing studied and concluded that sub-atmospheric regions and heat transfer coefficients peaks were co-related for low spacing.

A small number of studies dealing with jet impingement heat transfer on a rib fitted surface, experimentally or numerically, exist in the literature. Jet impingement on a rib fitted target surface disrupts the wall jet and thus level of turbulence and heat transfer are expected to increase [20]. Katti and Prabhu [21] studied the effect of rib height, width, pitch, clearance of the detached ribs from the flat plate and the location of the first rib from the stagnation point on local heat transfer. They observed continuous *Nu* augmentation from the stagnation point up to the first detached rib for all the configurations studied, due to an accelerated fluid in the stagnation zone by the clearance of the first rib. They also observed that the addition in the rib height may lead to reduction in *Nu* downstream from the first rib. Likewise Gau and Lee [22] observed that the flow features with rib-

roughened walls were different from the flat plate configuration with a reduced heat transfer near the impingement region. Subsequently Gau and Lee [23] experimentally studied jet impingement heat transfer on a triangular ribbed surface. They showed that air bubble formation in rib cavities near the stagnation point could reduce heat transfer, which sometimes could be smaller than that on a flat plate. But they showed that for more turbulent wall jet a significant enhancement in heat transfer with ribbed surface could be achieved. However if jet flow hits the ribbed surface containing large turbulence, e.g., with high *Re* or large *H/B* value, then the wall jet may possibly infiltrate the rib cavity and can effectively impinge on the surface with a subsequent reduction in the drag force due to rib projection. Thus an enhancement in heat transfer can be achieved [23]. Recently Tan *et al.* [24] experimentally investigated three rib configurations, namely, orthogonal, V-shaped and inverted V-shaped ribs with *H/B* values of 1 to 3 and *Re* from 6000 to 30000. They observed 30% enhancement in heat transfer with the rib roughened wall than that with a flat plate.

## 3. COMBINED EXPERIMENTAL AND COMPUTATIONAL STUDIES

Baydar and Ozmen [25] experimentally and numerically obtained the mean velocity, pressure distribution and turbulence intensity for *Re* ranging from 30000 to 50000 and *H/D* 0.2 to 6. Uncertainties involved in experimental results obtained were $\pm$2% in *Re*, $\pm$5% in axial velocity, $\pm$6% and $\pm$4% in turbulent velocities ($u'$ and $v'$), and $\pm$1% in the pressure measurements at the impingement plate. They concluded that turbulent intensity, heat transfer coefficients and sub-atmospheric region were linked together and found the predictions using the standard $k$-$\varepsilon$ model to be in best agreement with their experimental results for moderate *H/D* values. Fattah [26] experimentally and numerically studied a 2-D circular jet impingement flow without any cross flow. He considered jet *Re* from 95000 to 224000, *H/D* 3 to 12, jet angle $0^0$ to $20^0$ and nozzle to nozzle centerline spacings (*l/D*) of 3, 5 and 8. The accuracy in wall static pressure measurement was $\pm$3% and in temperature reading of $\pm 0.5^0$C. He observed a secondary stagnation point between the jets and a decreased pressure at this point by increasing the jet angle or decreasing *Re*.

Sagot *et al.* [27] experimentally and numerically studied the heat transfer configuration for a round jet impingement on a flat plate maintained at a constant wall temperature. They observed that the SST $k$-$\omega$ turbulence model performed well when local *Nu* was compared with the experimental data. Numerical results obtained with a constant wall temperature applied at the impingement wall were found to be in good agreement compared to a constant heat flux condition. Öztekin *et al.* [28] experimentally and numerically investigated the hydrodynamics of a slot jet impingement on concave flat surfaces. They carried out experiments for *Re* ranging from 3000 to 12500, *H/B* 1 to 14 and dimensionless curvature values (*R/L*) of 0.5, 0.5125, 0.566, 0.725 and 1.3 of impinging surface. They performed simulations with the $k$-$\varepsilon$ model for concave plate with dimensionless curvature value (*R/L*) = 0.725 and flat plate with enhanced wall functions. They observed a decreased value of the pressure coefficient at the stagnation point with *H/B* and variation of the local pressure coefficient computed with the standard $k$-$\varepsilon$ model with an enhanced wall treatment was in excellent agreement with the experimental data. Caggese *et al.* [29] investigated the heat transfer characteristics of fully confined jet impingement experimentally and numerically with low *H/D* values of 0.5 to 1.5 and *Re* in the range of 16500 to 41800. They observed significant effect of different separation distances on the flow field and hence it affected the distribution of heat transfer coefficient. Their numerical results showed satisfactory prediction of local and average Nusselt numbers.

## 4. COMPUTATIONAL APPROACHES USED FOR IMPINGING JETS

### 4.1 RANS computations

Majority of RANS based turbulence models considered in the literature did not predict impinging flows accurately and its complexities except a few [30-33]. Al-Sanea S [34] numerically investigated the heat transfer and flow characteristics of an impinging laminar slot jet. He observed identical results for free and semi confined jet impingements with a slight difference down the region due to entrainment effects. He also showed increased *Nu* with jet *Re* and *Pr* and it decreased with a reduction in the *H/B* value. They showed that the cross-flow effect can reduce the nominal *Nu* by as much as 60%. Further Sharif and Banerjee [35] numerically investigated heat transfer from a moving plate due to confined slot jet impingement. They specified 2% turbulence intensity at the jet exit and a length scale equal to 2*B* with constant pressure outlet condition to handle such complex flow situations due to plate movement.

Arquis *et al.* [36] computationally studied the flow and heat transfer features for cooling of an array of multiple protruding heated blocks using laminar slot jet and studied the effect of channel height, *Re*, slot width, spacing between blocks and height of blocks on heat transfer and fluid flow. They categorized the flow field with the presence of impingement flow and wall jet flow with possible survival of a primary circulation cell between the jet and confinement wall. They observed secondary circulation cells between the blocks, plus a secondary recirculation cell at the top surface of the downstream blocks. The strength and size of primary and secondary circulation cells and the flow separation (formation of recirculation cells) at the top surface of downstream blocks were found to increase with *Re*, channel height and decreasing slot width. These flow structures significantly affected the heat transfer characteristics. They also observed that cooling efficiency of all the blocks increased with *Re* and through reduction in slot width and channel height. But an increase in *Re* and channel height and reduction in slot width decreased the heat transfer rates from the downstream blocks because of the formation of recirculation cells at the top surface of these blocks. Dutta *et al.* [30] observed that the inflow turbulence intensity strongly affected the heat transfer distribution on the wall and the discretization scheme did not produce any significant difference in computed results for second or higher order scheme used. Some important literature dealing with RANS computations of jet impingement heat transfer with key parameters considered and observation made are summarized in Table 1.

**Table 1.** A summary of important RANS computations of jet impingement heat transfer

| Author(s) | Configuration and important parameters studied | Summary of important observations |
|---|---|---|
| Craft *et al.* [32] | Three different Reynolds-stress transport (RSM) models and a low-*Re* $k$-$\varepsilon$ model studied for round impinging jet at *Re* of 23000 and 70000. | Poor performance of the eddy-viscosity model and the basic RSM model. Inaccuracy of RSM was due to the use of the eddy viscosity model near the wall which could be removed by using a low-*Re* version of RSM. |
| Heyerichs and Pollard [37] | Wall functions and low-*Re* versions of $k$-$\varepsilon$ and $k$-$\omega$ models for impinging jet assessed. | Observed poor performance of the wall functions approach compared to low-*Re* model. The $k$-$\omega$ model performed superior than the $k$-$\varepsilon$ model. |
| Hofmann *et al.* [33] | Thirteen different RANS models tested for steady and pulsating impinging jets. | Observed that SST $k$-$\omega$ model can accurately predict the pulsating jets. |
| Wang and Majumdar [38] | Compared low-*Re* $k$-$\varepsilon$ models using the Yap correction in the dissipation ($\varepsilon$) equation for a turbulent slot jet. | Observed that the Yap correction reduced the turbulence length scale in the near wall region and thus it was found to over-predict the turbulence kinetic energy in the stagnation region. |
| Behnia *et al.* [31] | Studied axisymmetric isothermal fully developed turbulent jet impinging on a flat plate for fixed *Re* = 23000 and *H/D* = 0.5 - 14. | Predictions of local heat transfer coefficient with $v^2$-$f$ turbulence model were in excellent agreement with the experimental data while the $k$-$\varepsilon$ turbulence model over-predicted the flow features. |
| Behnia *et al.* [39] | Turbulent heat transfer in confined and unconfined axisymmetric impinging jets with wide range of *Re* and *H/D*. | $v^2$-$f$ turbulence model showed an excellent agreement with experimental data. They also observed strong effect of turbulence intensity and velocity profile on *Nu* distribution. |
| Yang and Tsai [40] | High turbulence air jet impingement on a circular disk with low-*Re* $k$-$\omega$ turbulence model with *Re* = 16100 to 29600 and *H/D* = 4 to 10. | *Re* has a considerable effect on the flow field and heat transfer. They observed that high value of turbulence in the jet leads to higher heat transfer coefficients in the stagnation zone. |
| Draksler and Koncar [41] | Studied local heat transfer and flow field characteristics for axis-symmetric impinging jet with eddy viscosity based SST turbulence model. | RANS computations of local and average heat transfer predictions were satisfactorily accurate. They observed that chamfering the edges of nozzle inlet resulted in a reduction in the heat transfer and pressure drop. |
| Yang *et al.* [42] | Flow and heat transfer features for slot jet impinging on a semi-circular concave surface with $k$-$\varepsilon$ model for *Re* = 5920 - 23700 and *H/B* = 0.5 - 12. | Maximum *Nu* occurred at the stagnation point and predicted local *Nu* were in good agreement with the experimental data with a maximum deviation of 15%. |
| Dutta *et al.* [30] | Compared various RANS models for prediction of flow field and heat transfer for slot jet impinging flows with *Re* = 20000 and *H/B* = 4 and 9.2. | Standard and SST $k$-$\omega$ models with transitional model for low *H/B* value and standard $k$-$\varepsilon$ models for high *H/B* value were found to be in best agreement with the experimental data. |
| Sharif and Banerjee [35] | Heat transfer from a moving plate for 2-D slot jet studied with standard $k$-$\varepsilon$ turbulence model and RSM model with enhanced wall treatment for *Re* = 5000 to 20000, *H/B* = 6 to 8. | Significant increment in average *Nu* with jet *Re* and plate velocity (normalized with jet exit velocity and varied in the range 0 to 2). The average skin friction coefficient was found comparatively unaffected with *Re* but it increased with the velocity of plate. |
| Xu *et al.* [43] | Heat transfer enhancement with turbulent impinging jet due to intermittent pulsation with 2-D symmetric slot jet configuration studied with uniform velocity profile applied at the jet inlet. | Heat transfer rate was significantly dependent on progresses of thermal and hydrodynamic boundary-layers with time. They showed considerable enhancement in heat transfer by the intermittent pulsation. Further they observed significant effect of on-off jet time ratio and *H/B* on heat transfer rate. |
| Pakhomov and Terekhov [44] | Fluid flow and heat transfer characteristics for an intermittent turbulent impinging round jet. They carried out simulation for steady state and intermittent cases both with Reynolds stress transport model. | They reported reduction in heat transfer with an increase in *Re* such that the pulsed case turned approximately into a steady state one. They observed increased *Nu* with an increment in pulse frequency ($f$ < 150 Hz) and at small frequencies ($f$ < 30 Hz). |
| Dutta *et al.* [45] | Slot jet impingement heat transfer with nano fluid ($Al_2O_3$-water). The standard $k$-$\varepsilon$ model, SST $k$-$\omega$ model and $v^2$-$f$ model were used for computation. | The average heat transfer coefficient at the impingement plate was observed to be approximately 27% and 22% for laminar and turbulent slot jet impingement, respectively. However the pumping power was found to increase by five times. |

### 4.2 LES and boundary conditions

Many authors, such as, Cziesla *et al*. [46]**,** Uddin *et al.* [47], Dutta *et al.* [48], Dairay *et al.* [49] and Dutta *et al.* [50] observed that LES can predict the flow field and heat transfer data within the accepted accuracy limits. Development of LES wall functions for computation is quite important for impinging flows [1]**.** Cziesla *et al.* [46] considered periodic boundary condition along the width (equal to two slot widths), height of 8*B* - 12*B* (spacing between nozzle to plate) and length 10*B* of the domain. Beaubert and Viazzo [51] suggested that the length of the computational domain in the horizontal direction must be large enough to capture two big recirculations on both sides of jet and showed that $x/B = \pm 40$ is sufficient. Similar to Cziesla *et al.* [46], they also considered the periodic boundary along the width of the domain and suggested that this dimension should be large enough to capture the biggest structures of the flow in order to justify the periodic conditions.

Chattopadhyay and Saha [52] investigated the flow field and heat transfer in a rectangular slot jet, impinging on moving surface and the velocity of the impinging plate was

varied two times the jet exit velocity. They considered various turbulence quantities. Icardi *et al.* [53] predicted turbulent flow field in a 3-D confined impinging jets reactor (CJIR) with different SGS models and boundary conditions. They observed a good agreement for mean and fluctuating velocity predictions and the effect of sub-grid scale model was found to be insignificant for low to moderate values of *Re*. They suggested that LES can be used rather than expensive DNS and micro PIV experiments to obtain fast and consistent data.

**Table 2**. A summary of important LES computations of jet impingement heat transfer

| **Author(s)** | **Configuration and important parameters studied** | **Summary of important observations** |
|---|---|---|
| Gao and Voke [54] | Instantaneous thermal distribution with simple SGS model at *Re* = 6500 and with different fluid properties. | Observed that for jets with cool edges and hot core, the cooled fluid accumulated in the recirculation regions, but the hot fluid spread over the plate as the jet impinged. |
| Voke and Gau [55] | Plane water jet impinging normally on a plate examined at *Re* = 6500 and with Smagorinsky SGS model. | Proposed that the simple 1-D conduction model is capable of computing the near wall thermal behavior. |
| Olsson and Fuchs [56] | LES of semi-confined circular impinging jet at *Re* = 10000 with both dynamic and similarity SGS models. | Influence of SGS model on velocity field was assessed. They reported that similarity model performed better than the dynamic model at sufficient resolution. |
| Cziesla *et al.* [46] | Flow field and heat transfer for an impinging jet emanating from a rectangular slot nozzle at *Re* = 2000 - 10000 with dynamic SGS model. | The model was capable of predicting the turbulent production rate. They observed negative turbulent kinetic energy production rate close to the wall and jet centerline and a better accuracy in the heat transfer predictions at the stagnation region. |
| Tsubokura *et al.* [57] | Compared 3-D eddy structures for both plane and round impinging jets at *Re* = 6000 and with dynamic SGS model. | Twin vortices were observed in the impingement region of plane jet. They also observed non organized structures in the stagnation region for round jet. |
| Beaubert and Viazzo [51] | Plane jet impingement using the dynamic Smagorinsky model at *Re* = 3000 to 13500. | The wall shear stress at the impingement wall and effect of *Re* on the kinematic expansion of the jet were analyzed. |
| Beaubert and Viazzo [58] | Examined the influence of *Re* on structure of a plane jet at *Re* = 3000 and 7500 using dynamic SGS model. | Counter-rotating cells were observed near the impingement zone. |
| Chattopadhyay and saha [52] | Investigated the flow field and heat transfer emanating from a rectangular slot jet impinging on moving surface at *Re* = 5800 using dynamic SGS model. | They observed increment in the turbulent kinetic energy with impinging surface velocity. Turbulence production rate increased primarily with the increment in the surface velocity and thereafter it came down. |
| Mingzhou *et al.* [59] | Flow field of a semi-confined rectangular exit turbulent impinging jet, on a flat surface at *Re* = 8500 and with dynamic SGS model. | They observed that the secondary vortices generated in the wall jet region were due to the periodic advancement of the primary vortex structure. |
| Hadžiabdić and Hanjalić [60] | Studied the vortical and turbulence structures with the local heat transfer in impinging flow with *Re* = 20000 using dynamic SGS model. | Their LES data provided clarifications for some of the experimentally noticed flow features, e.g., secondary peak in *Nu* and the negative turbulence energy production in the stagnation region. |
| Rhea *et al.* [61] | Investigated the single phase jet impingement with RANS and LES computations at *Re* = 10000 using dynamic SGS model. | Observed some under-production of turbulence quantities by the RANS computations in critical regions, e.g., in free and wall jet regions, the LES computations showed close agreement with the experimental data, particularly in critical zones. |
| Uddin et al. [62] | LES of an impinging jet to provide suitable data for validation of mathematical models at *Re* = 23000 using dynamic SGS model. | Mean, turbulent flows and turbulent heat flux were calculated for the assessment of three turbulent heat flux models for predicting round impinging jets. |
| Lodato *et al.* [63] | Studied wall jet interaction with mixed similarity and WALE models at *Re* = 23000 and 70000. | Compared to standard WALE, mixed similarity model showed significant improvement in the prediction of the second order moments. |
| Uddin *et al.* [47] | Dynamic Smagorinsky model was used to obtain the flow field and heat transfer characteristics of jet impingement at *Re* = 13000 and 23000 and jet to plate spacing (*H/D*) of 2. | They observed that LES computations of impinging jet were extremely sensitive to the quality of the grids linked with different zones. They observed intermittent ring of vortex generation when jet struck the surface. |
| Dutta *et al.* [48] | Fluid flow and heat transfer of a turbulent slot jet impingement at *Re* = 13500 and *H/B* of 10 with dynamic SGS model. | They showed that peaks of Nusselt number and turbulence kinetic energy coincided and concluded that the turbulence plays an important role in wall heat transfer. |
| Dairay *et al.* [49] | Computed turbulent jet impinging on a heated wall at *Re* of 10000 and *H/D* = 2. | They concluded that in more realistic situation, increase of spatial resolution of LES resulted in capturing more correct flow feature and hence the secondary peak in Nusselt number. |

Table 2 presents review of important literature dealing with LES of jet impingement heat transfer with their key observations and numerical challenges. Uddin *et al.* [47] performed LES using second order accurate schemes for space and time discretizations and observed that the flow acceleration in the developing zone of the boundary-layer was linked to the secondary peak observed in the radial distribution of *Nu*. Dairay *et al.* [49] computed turbulent jet impinging on a heated wall with LES using higher order numerical scheme and performed DNS for *Re* = 10000 and *H/D* = 2. They used DNS results as a reference to compare two LES computations, one based on the hypothesis of conventional eddy viscosity and the other on high order numerical dissipation. Both LES computations were found to

be acceptable in predictions of velocity statics compared to DNS and experimental data. They observed that the conventional eddy viscosity based sub-grid scale model (dynamic Smagorinsky and WALE) did not control numerical errors at small scale, which led to unrealistic predictions of heat transfer in the impingement zone. They also observed that strong nonlinearities present in the expressions for dynamic Smagorinsky and WALE models were a substantial source of error generation. Dutta *et al.* [48] used two inflow conditions, i.e., one with no inflow fluctuations and the other with fluctuations. They observed that LES results without any inflow fluctuations were in good agreement with the experimental data for the predictions of mean flow, turbulence intensity and heat transfer on the impingement wall.

### 4.3 DNS and hybrid approaches

DNS can be applied to simple geometries with low *Re* [64 - 66]. Hattori and Nagano [65] carried out DNS and observed the effects of nozzle to plate spacing. They observed a secondary peak in the local *Nu* in the wall jet developing region for low *H/B* value and showed larger wall normal turbulence intensity close to the wall in the wall jet region and hence a secondary peak in *Nu* occurred. They also observed a secondary peak in the skin friction coefficient in case of low *H/B* value similar to that of local heat transfer.

Jaramillo *et al.* [66] performed DNS and RANS computations in order to assess the flow field and heat transfer characteristics of plane impinging jets with *Re* = 20000 and *H/B* = 4. They used DNS results reference data to assess the performance of several RANS based models. They considered periodic boundary condition in the span-wise direction and turbulent length scale of 0.015*B* at the inlet and suggested that the outflow should be placed at least at 40*B* to capture main recirculating flow from the jet centreline. They showed that DNS produced noteworthy outcome on the local heat transfer upon changing the boundary condition at the impingement wall from a constant heat flux to a constant temperature.

Kubacki and Dick [67] simulated plane impinging jets using the *k-ω* based hybrid RANS/LES and *k-ω* RANS models with *H/B* = 10, 9.2 and 4 and *Re* from 13500 – 20000. They set $\pi B$ as the size of the domain in the span-wise direction and applied periodic boundary and turbulent length scale at the inlet was set as 0.015*B* and observed that the hybrid models predicted the wall shear stress and heat transfer rate on the impingement plate in much better way than by the *k-ω* RANS model. They also observed that the hybrid model was capable of resolving the evolution of the large scale structures originating at the jet exit and its destruction in to smaller scales. Further Kubacki and Dick [68] simulated the flow and convective heat transfer characteristics of round impinging jets for different set of *H/D* of 2, 6 and 13.5 and *Re* of 5000, 23000 and 70000. They tested the *k-ω* model with three hybrid RANS/LES models and observed that the turbulence kinetic energy was over-predicted at low value of *H/D* computed by RANS model. For high *H/D* value the turbulence mixing was under-predicted by RANS model in the shear layer and thus length of the potential core became too large and therefore heat transfer results were also over-predicted. They observed that all hybrid RANS/LES models produced better result by improving over- and under-predictions of RANS model.

Kubacki *et al.* [69] studied the capability of hybrid RANS/LES computations of jet impingement with Detached Eddy Simulation (DES) and Partially-Averaged Naiver Stokes (PANS) model for two configurations, i.e., *H/B* = 10, *Re* = 13500 and *H/B* = 4, *Re* = 20000. They considered the outflow boundary condition at $X = \pm 40B$, periodic boundary condition in the span-wise direction (width equal to $\pi$) and turbulent length scale as *0.1667B*. For DES the turbulent length scale was substituted by the grid size in the eddy viscosity formulation and in the destruction term of *k*-equation and for PANS it was substituted from the sub-filter dissipation rate and total turbulence kinetic energy. They observed that the hybrid models in contrast to RANS models were capable of replicating the turbulent flow dynamics of the impinging jet in the shear layer. They observed that the prediction of the skin friction was better with DES than with PANS. Taghinia *et al.* [70] performed CFD study of twin jet impingement using hybrid RANS-LES model. They applied the SST-SAS *k-ω* (shear stress transport with scale-adapted simulation) model with hybrid (RANS/LES) feature for turbulence modeling. They observed that the SST-SAS model can predict reasonably accurate results particularly for low *H/B* value and showed accurate prediction of the peak value of *Nu* by the SST-SAS model.

## 5. IMPORTANT REVIEWS ON JET IMPINGEMENT HEAT TRANSFER

Zuckerman and Lior [20] described the physics, correlations and numerical simulation techniques for jet impingement heat transfer. They studied various turbulence models, namely, *k-ε*, *k-ω*, RSM, algebraic stress, SST and $v^2$-*f*, to identify methods to predict with their drawbacks and suitability. They observed that the SST and $v^2$-*f* models provided the best result in small computation times. Jambunathan *et al.* [71] reviewed the experimental data of heat transfer available for single circular impinging turbulent jets and considered *Re* in range of 5000 to 124000 and *H/D* 1.2 to 16. Based on the assessment of the empirical results they showed *Nu* as a function of *Re*, axial distance, *H/D* and *Pr*. They also showed that *Nu* in the wall jet region was independent of *H/D* in the range of 1 to 12 for circular jets.

Viskanta [72] considered both slot and circular jets and effect of cross flow on jet impingement heat transfer. He emphasized on physical phenomenon involved in impingement heat transfer for all the cases considered. He summarized the effect of various factors for single and multiple gas jets, such as, turbulence in jet, geometric effects, jet outlet conditions, angle of incidence, curvature surfaces and various other external factors on impingement heat transfer enhancement. He observed that for single impinging jet the maximum heat transfer occurred at the end of the potential core (nearly 6 diameters downstream). Zukerman and Lior [73] carried out a concise review of accuracy and shortcomings associated with numerical methods used to predict flow field and heat transfer characteristics of jet impingement and showed that *k-ε*, *k-ω*, ASM and RSM models provided poor results compared to experimental data even with high resolution grids. The SST and $v^2$-*f* RANS models produced better prediction of flow field and heat transfer characteristics. Dewan *et al.* [1] presented a review of computational status of turbulent jet impingement heat transfer. They reviewed SGS models, inflow and other

boundary conditions associated with different LES studies and concluded that the accuracy of different LES computations cannot be judged because of a lack of the generalization in the reported LES data.

Some key conclusions that can be drawn from the literature review presented here are as follows. Jet impingement heat transfer configuration is widely studied by many researchers, both experimentally and computationally. Several parameters were found to affect its flow features and heat transfer characteristics, such as, flow confinement, nozzle shape, jet to plate spacing and *Re*. These parameters have found special attention in the literature either experimentally or numerically. Low nozzle to plate spacing configuration was less studied computationally with LES or hybrid models. Some authors, such as, Chung *et al*. [64] and Jaramillo *et al.* [66], showed that DNS can be applied to simple geometries with low *Re* but its result can be used as a reference as the use of DNS is much more expensive than LES. Further, some hybrid models are needed that can predict the fluid flow and heat transfer characteristics within the acceptable accuracy limits [73]. Recently some authors [67-69] have used hybrid models, such as, PANS, DES, etc., and concluded that these models provide reasonably accurate result and were found to be less computationally expensive than LES and DNS. Hence some of hybrid models, such as, PANS and DES, may be used to obtain a suitable compromise between the accuracy and cost of solution.

A small number of studies dealing with application based jet impingement heat transfer configuration, e.g., ribs fitted impingement plate, moving impingement plate, etc., experimentally or numerically have been reported in the literature. Pulsating inlet flow jets produce large scale eddies in the vicinity of jet exit, which cause unsteady boundary-layers on the impingement plate. This behavior may change the heat transfer and flow features of jet impingement on a surface and it depends on the frequency of flow pulsation, *Re* and other dimensions [20]. Jet impingement on a rib fitted target surface disrupts the wall jet. Hence level of turbulence is expected to increase and consequently the heat transfer. But the use of ribs increases the drag force and the wall jet decelerates and disappears rapidly. This effect needs to be analyzed in details [20].

## 6. COMPUTATIONAL DOMAIN AND BOUNDARY CONDITIONS

Fig. 2 shows details of the computational domain that can be considered to study jet impingement on flat and ribbed surfaces [30, 46, 67, and 69]. The no slip boundary condition can be applied at all walls (confined wall, impingement wall and ribs). A constant heat flux or constant temperature can be applied at the impingement plate. Fully developed flow or velocity profile observed in experiments can be applied at the nozzle exit with the specification of the nozzle exit velocity *U* based on *Re* with turbulence intensity (*I*) and turbulent length scale. The outflow boundary conditions were applied in the reported studies at sufficiently large distance to avoid a reversed flow. Periodic boundary conditions were applied at $Z = 0, W (W = \pi B)$ [67]. It is quite important to design a grid that offers an appropriate compromise between accuracy and computational cost. Grid should be finer at critical regions, such as, near the impingement and ribbed surfaces (at separation and reattachments), etc. Various initial and boundary conditions used by different researchers are as follows.

- Sharif and Banerjee [35] specified 2% turbulence intensity at the jet exit and a length scale equal to 2*B*.
- Cziesla *et al.* [46] and Beaubert and Viazzo [51] considered periodic boundary along the width (equal to two slot widths).
- Beaubert and Viazzo [51] suggested that the length of the computational domain in the horizontal direction must be large enough to capture two big recirculation regions on both sides of jet and showed that $H/B = 40$ is sufficient for LES.
- Kubacki and Dick [67] set $\pi B$ as the size of the domain in the span-wise direction and applied periodic boundary condition. The turbulent length scale at the inlet was set as 0.015*B*.
- Kubacki *et al.* [69] considered the outflow boundary condition at $X = \pm 40B$, periodic boundary condition in the span-wise direction (width equal to $\pi$) and turbulent length scale as *0.1667B*.

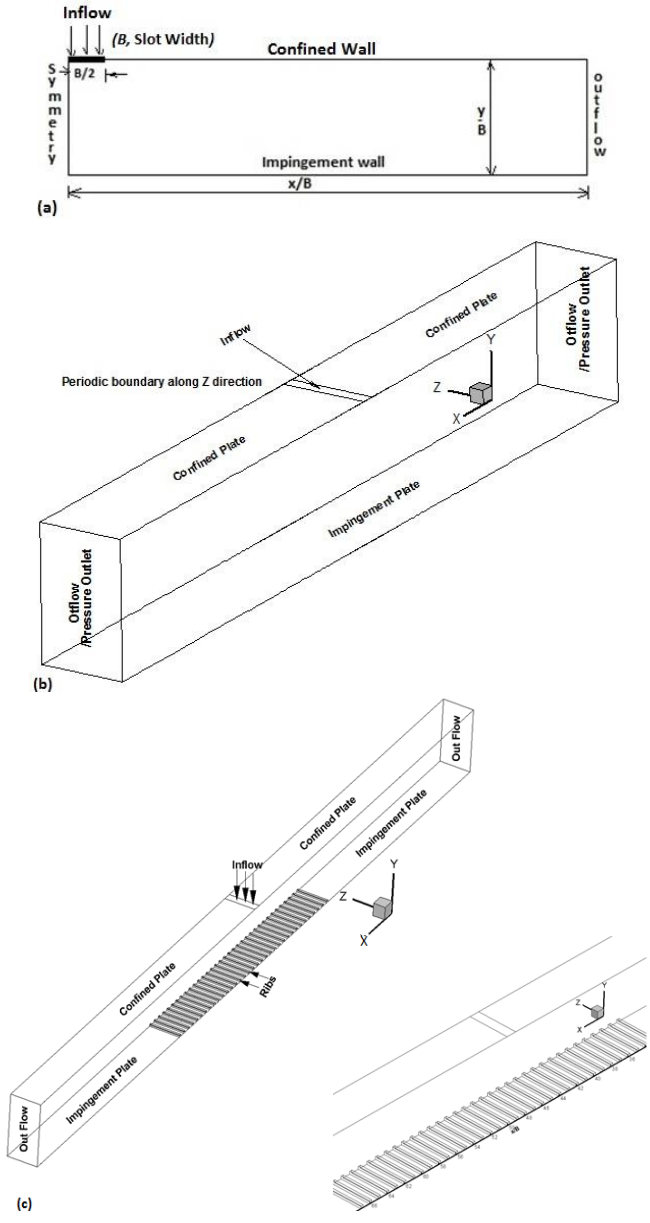


**Figure 2.** Details of (a) 2-D computational domain and (b, c) 3-D computational domain of jet impingement over flat and ribbed surfaces

An extremely small number of studies dealing with jet impingement heat transfer on a ribbed surface either experimentally or numerically have been reported. Different kinds of turbulent promoter surfaces and arrangements have been used in the literature for convective heat transfer enhancement [21-23, 74-77]. Two arrangements for rib roughened impingement surface are possible, e.g., ribs may be attached with the impingement surface [22, 23, 74, 78] (attached ribs) or these may be detached from the impingement surface with a small spacing between rib and impingement wall [21] (Fig. 3). Jet impingement on a ribbed surface disrupts the wall jet and flow separation and reattachment takes place due to rib projection. Thus level of turbulence and hence the heat transfer are expected to increase on a ribbed surface [Fig. 3 (c)]. Some application may be found in agriculture field for water jets. Understanding of thermal and fluid dynamic performance of a water droplet travelling from the nozzle outlet is quite important for its application area, such as, sprinkler used for irrigation in agriculture field to save water [79]. Such application of sprinkler jet can also be seen in [80] for classic quantum description used for single and multi-droplets. However we have not considered this topic in detail as here our focus is on jet impingement heat transfer.

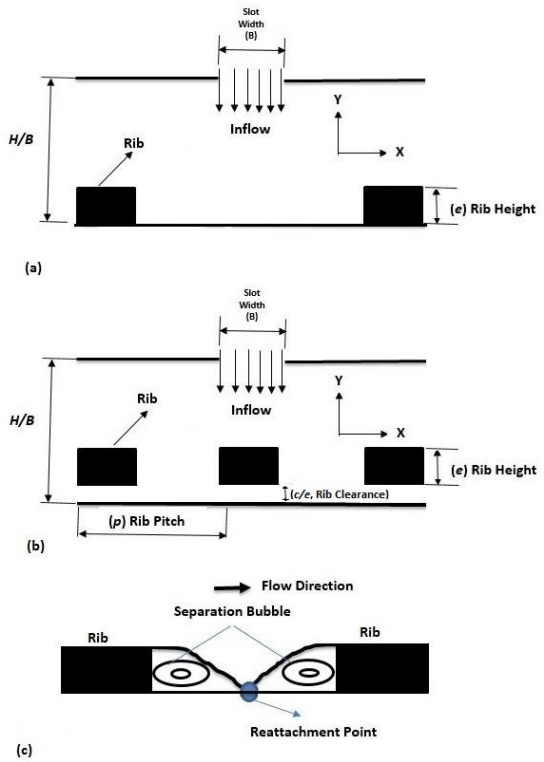


**Figure 3.** (a, b and c) Different arrangements of ribs on impingement surface

## 7. DIFFERENT COMPUTATIONAL APPROACHES USED FOR JET IMPINGEMENT

The Navier-Stokes (N-S) equations for instantaneous incompressible flow and without body forces can be written as:

$$\frac{\partial u_i}{\partial t} + u_j \frac{\partial u_i}{\partial x_j} = -\frac{\partial p}{\partial x_i} + \nu \frac{\partial^2 u_i}{x_j x_j} \quad (1)$$

$$\frac{\partial u_i}{\partial x_i} = 0 \quad (2)$$

Table 3 shows various techniques that can be used for computation of turbulent flows. For RANS computations, the time-averaged governing equations are solved. In DNS, unsteady, 3D Navier-Stokes equations for instantaneous flow are solved numerically and all temporal and spatial scales need to be resolved. In LES, unsteady, filtered governing equations are solved and the effect of small scales are considered using suitable subgrid scale (SGS) models.

**Table 3.** Various techniques used for computation of turbulent flows

| | **DNS** | **LES** | **RANS** |
|---|---|---|---|
| **Governing Equations** | Original Navier-Stokes (N-S) equations | Filtered N-S equations | Time averaged N-S equations |
| **Velocity field** | Three-dimensional and unsteady | Three-dimensional and unsteady | Steady/unsteady |
| **Modeling** | No modeling | Only small scales are modeled | All scales are modeled |
| **Cost of computations for flow over an airliner (Spalart [81]) in terms of number of grid points x number of time steps** | Most expensive, $10^{24}$ | Between DNS and RANS, $10^{18}$ | Least expensive $10^{7}$ (3D, steady) |
| **Application** | Simple geometries at low *Re* | High potential for practical as well as fundamental use. | Widely used in practice. |

The instantaneous velocity component can be decomposed as follows (with different meanings for RANS, PANS and LES)

$$u_i(x,t) = \overline{U}_i(x,t) + u'_i(x,t) \quad (3)$$

Similarly temperature can also be decomposed into its resolved and unresolved components

$$T(x,t) = \overline{T}(x,t) + T'(x,t) \quad (4)$$

### 7.1 Reynolds-averaged Navier-Stokes (RANS) equations

Many researchers have used RANS approach for impinging jet computation [30-33, 37, 82]. In the Reynolds-averaged Navier-Stokes (RANS) equations, the time-averaged Navier-Stokes equations are numerically solved.

The instantaneous velocity field can be decomposed into its mean (time-averaged) $\overline{U}_i$ and fluctuating components ($u'_i$) (Eq. 3), such that $\overline{u'_i} = 0$. Thus, the time averaging of the Navier-Stokes equations leads to extra terms, known as the Reynolds stresses, which need to be modelled. This results in a closure problem which require some approximation. The time-averaged governing equations for the conservations of mass, momentum and energy can be written as:

$$\frac{\partial \rho}{\partial t} + \rho \frac{\partial \bar{u}_i}{\partial x_i} = 0 \tag{5}$$

$$\frac{\partial \bar{u}_i}{\partial t} + \bar{u}_j \frac{\partial \bar{u}_i}{\partial x_j} = -\frac{1}{\rho}\frac{\partial \bar{p}}{\partial x_i} + \frac{1}{\rho}\frac{\partial}{\partial x_j}\left(2\mu \bar{S}_{ij} - \rho\overline{u'_i u'_j}\right) \tag{6}$$

$$\frac{\partial \bar{T}}{\partial t} + \bar{u}_j \frac{\partial \bar{T}}{\partial x_j} = \frac{1}{\rho}\frac{\partial}{\partial x_j}\left(\frac{\kappa}{c_p}\frac{\partial \bar{T}}{\partial x_j} - \rho\overline{u'_i T'}\right) \tag{7}$$

where, $\bar{S}_{ij} = \frac{1}{2}\left(\frac{\partial \bar{u}_i}{\partial x_j} + \frac{\partial \bar{u}_j}{\partial x_i}\right)$.

Here the term $(-\rho\overline{u'_i u'_j})$ in equation (6) is the Reynolds stress. Various turbulence models can be used. Most of the models are based on the Boussinesq approximation, which relates the Reynolds stresses to the mean velocity gradients as:

$$-\rho\overline{u'_i u'_j} = 2\mu_t \bar{S}_{ij} - \frac{2}{3}\rho k \delta_{ij} \tag{8}$$

where $k$ denotes the turbulence kinetic energy defined as $k = \frac{1}{2}\overline{u'_i u'_i}$, $\delta_{ij}$ denotes the Kronecker delta where $\delta_{ij} = 1$ if $i = j$ and $\delta_{ij} = 0$ if $i \neq j$ and $\mu_t$ the turbulent or eddy viscosity. Turbulent transport of heat is modeled in the same way as that for momentum

$$-\rho\overline{u'_i T'} = \frac{\mu_t}{Pr_t}\frac{\partial \bar{T}}{\partial x_i} \tag{9}$$

The turbulent Prandtl number ($Pr_t$) is defined as the ratio of the turbulent viscosity ($\mu_t$) and turbulent thermal diffusivity ($\Gamma_t$) and is given as: $Pr_t = \frac{\mu_t}{\Gamma_t}$.

A typical value of the turbulent Prandtl number used in engineering computations is approximately equal to 1 [83]. Readers are referred to any book or paper for details on turbulence model used in the literatures, such as [30, 83, 84].

Turbulent models are categorized on the basis of the number of differential transport equations employed to determine the turbulent viscosity ($\mu_t$) and these can be broadly classified as

- Algebraic (zero-equation) models
- One-equation models
- Two-equations models
- Reynolds stress-transport models

### 7.2 Large eddy simulation

Many researchers have used LES for impinging jet computation [46-50]. Large eddy simulation (LES) is a computation in which the large eddies are computed and the effect of the smaller eddies, termed as the subgrid-scale (SGS), are modeled. This approach is used because the largest eddies are directly affected by the boundary conditions and flow domain, carry most energy, and must be computed. On the other hand, the small-scale eddies are isotropic in nature, contribute less to Reynolds stresses, carry small energy and therefore are less critical. Also, small eddies have nearly-universal characteristics and therefore are easy to model (Wilcox [84]). Thus, a coarser grid and much larger time steps can be used in a LES compared to DNS.

In LES, a filtering operation is performed over the governing equations, in which velocity $u$(x,t) is decomposed into resolved $\overline{U}_i$(x,t) and unresolved $u'$(x,t) components (Eq. 1). The filtered velocity is defined as:

$$\bar{U}_i(x,t) = \int G(x,x')u_i(x',t)dx'$$

where the function $G(x,x')$ denotes the filter kernel.

The filtering operation of the continuity and Navier-Stokes equations provides almost similar forms as Eqs. (5) and (6). The resulting momentum equation is closed by modeling the viscous tensor, $\tau_{ij}$ which can be defined using the Smagorinsky model as:

$$\tau_{ij} = -2\mu_t \overline{S_{ij}}$$

where $\overline{S_{ij}}$ denotes the rate of stress tensor for the resolved scale. The turbulent viscosity ($\mu_t$) is a function of density (ρ), filter width (Δ) and characteristic filtered rate of strain ($\bar{S}$). It is defined as:

$$\mu_t = C_s^2 \rho \Delta^2 |\bar{S}|$$

where $C_s$ is an empirical constant.

Subgrid stress model (SGS) is used in LES to consider the interactions between the resolved and unresolved scales. More specifically SGS models are used to consider the subgrid stress term ($\tau_{ij}$) in the filtered governing equations. Although, SGS models are often compared with RANS based turbulence models, the way in which the Reynolds averaging is defined is different from the filtering approach in LES. Moreover, since small scales are generally assumed to be isotropic and universal, SGS models are fairly easy to model and are accurate as compared to RANS based turbulence models. SGS models are of two types, i.e., similarity and eddy-viscosity models. The eddy viscosity models are more popular than similarity models.

### 7.3 Partially-averaged Navier-Stokes (PANS) Modeling

Some researchers have used the PANS approach for impinging jet computations [68, 69] which employs unsteady, filtered governing equations. The PANS equations [85] vary smoothly from RANS equations to Navier-Stokes equations (direct numerical simulation), depending on the values of the filter-width control parameters, $f_k$ and $f_\varepsilon$. Here $f_k$ is the ratio of the unresolved turbulence kinetic energy ($k_u$) to total kinetic energy ($k$) and $f_\varepsilon$ is the ratio of unresolved dissipation rate ($\varepsilon_u$) to total dissipation rate ($\varepsilon$).

$$f_k = \frac{k_u}{k}; \quad f_\varepsilon = \frac{\varepsilon_u}{\varepsilon}$$

In the PANS approach, the extent of filtering is quantified by specifying the values of $f_k$ and $f_\varepsilon$. It is well known that much of the kinetic energy is contained in large scales and most of the dissipation occurs in the smallest scales due to which $0 \leq f_k \leq f_\varepsilon \leq 1$. Smaller the value of $f_k$ higher the physical resolution: $f_k = 1$ represents RANS and $f_k = 0$ indicates DNS. Authors may find detailed formulation of PANS in [85].

## 8. CONCLUSIONS

A comprehensive review of jet impingement heat transfer has been presented. The review includes different physical and computational aspects of impinging flows. Studies dealing with application based jet impingement heat transfer configuration have also been reviewed. Jet impingement heat transfer is widely studied experimentally by many researchers. Although it is also extensively studied computationally by many researchers, it is clear that majority of RANS turbulence models did not predict impinging flows accurately and its complexities. Several parameters affect the flow and heat transfer characteristics of jet impingement and these have found special attention in the literature experimentally and numerically. It can be observed that for low nozzle to plate spacing reason for appearance of secondary peak in Nusselt number still needs to be addressed. Many authors have observed that LES is capable of predicting the flow and heat transfer characteristics within the accepted accuracy limits. DNS can be applied to simple geometries with low values of *Re*. Recently some researchers have used hybrid models, such as, PANS, DES, etc., and concluded that these models provide reasonably accurate results and were less computationally expensive than LES and DNS. Some studies dealing with application based jet impingement heat transfer configuration (e.g., ribs fitted impingement plate, moving impingement plate, etc.) have been reported in the literature. It has been observed that jet impingement on a rib fitted target surface disrupts the wall jet and boosts the turbulence level through better mixing of fluid and hence heat transfer enhancement can be achieved through it.

## ACKNOWLEDGMENT

The work reported here forms a part of the Department of Science and Technology (DST), Government of India, New Delhi, sponsored project (SR/S3/MERC/0114/2012). Authors acknowledge the financial support received from DST.

## REFERENCES

[1] Dewan A., Dutta R., Srinivasan B. (2003). Recent trends in computation of turbulent jet impingement heat transfer, *Heat Transfer Engineering*, Vol. 33, No. 4-5, pp. 447-460. DOI: 10.1080/01457632.2012.614154

[2] Livingood J.N.B., Hrycak P. (1973). Impingement heat transfer from turbulent air jets to flat plates: a literature survey, Security. X-2778, 43.

[3] Ashforth-Frost S., Jambunathan K., Whitney C.F. (1997). Velocity and turbulence characteristics of a semiconfined orthogonally impinging slot jet, *Experimental Thermal and Fluid Science*, Vol. 14, No. 1, pp. 60–67, 1997. DOI: 10.1016/S0894-1777(96)00112-4.

[4] Schlichting H. (1968). *Boundary-Layer Theory*, McGraw-Hill, New York.

[5] Hoogendoorn C.J. (1977). The effect of turbulence on heat transfer at a stagnation point, *International Journal of Heat and Mass Transfer*, Vol. 20, No. 12, pp. 1333–1338. DOI: 10.1016/0017-9310(77)90029-1.

[6] Ashforth-Frost S., Jambunathan K. (1996). Effect of nozzle geometry and semi-confinement on the potential core of a turbulent axisymmetric free jet, *International Communications in Heat and Mass Transfer*, Vol. 23, No. 2, pp. 155–162. DOI: 10.1016/0735-1933(96)00001-2.

[7] Zhe J., Modi V. (2001). Near wall measurements for a turbulent impinging slot jet, *Journal of Fluids Engineering*, Vol. 123, No. 1, pp. 112–120, 2001. DOI: 10.1115/1.1343085.

[8] Gardon R., Akfirat J.C. (1965). The role of turbulence in determining the heat-transfer characteristics of impinging jets, *International Journal of Heat and Mass Transfer*, Vol. 8, No. 10, pp. 1261–1272. DOI: 10.1016/0017-9310(65)90054-2.

[9] Koopman R.N.N., Sparrow E.M.M. (1976). Local and average transfer coefficients due to an impinging row of jets, *International Journal of Heat and Mass Transfer*, Vol. 19, No. 6, pp. 673–683. DOI: 10.1016/0017-9310(76)90051-X

[10] Baines W.D., Keffer J.F. (1976). Shear stress and heat transfer at a stagnation point, *International Journal of Heat and Mass Transfer*, Vol. 19, No. 1, pp. 21–26. DOI: 10.1016/0017-9310(76)90006-5

[11] Lytle D., Webb B.W. (1994). Air jet impingement heat transfer at low nozzle-plate spacings, *International Journal of Heat and Mass Transfer*, Vol. 31, No. 12, pp. 1687–1697. DOI: 10.1016/0017-9310(94)90059-0

[12] Tu C.V., Wood D.H. (1996). Wall pressure and shear stress measurements beneath an impinging jet, *Experimental Thermal and Fluid Science*, Vol. 13, No. 4, pp. 364–373. DOI: 10.1016/S0894-1777(96)00093-3

[13] Maurel S., Solliec C. (2001). A turbulent plane jet impinging nearby and far from a flat plate, *Experiments in Fluids*, Vol. 31, No. 6, pp. 687–696. DOI: 10.1007/s003480100327

[14] O'Donovan T.S., Murray D.B. (2007). Jet impingement heat transfer - Part I: Mean and root-mean-square heat transfer and velocity distributions, *International Journal of Heat and Mass Transfer*, Vol. 50, No. 17, pp. 3291–3301. DOI: 10.1016/j.ijheatmasstransfer.2007.01.044

[15] O'Donovan T.S., Murray D.B. (2007). Jet impingement heat transfer - Part II: A temporal investigation of heat transfer and local fluid velocities, *International Journal of Heat and Mass Transfer*, Vol. 50, No. 17, pp. 3302–3314. DOI: 10.1016/j.ijheatmasstransfer.2007.01.047

[16] Alekseenko S.V., Bilsky A.V., Dulin V.M., Markovich D.M. (2007). Experimental study of an impinging jet with different swirl rates, *International Journal of Heat and Fluid Flow*, Vol. 28, No. 6, pp. 1340–1359. DOI:

10.1016/j.ijheatfluidflow.2007.05.011
[17] Bakirci K., Bilen K. (2007). Isualization of heat transfer for impinging swirl flow, *Experimental Thermal and Fluid Science*, Vol. 32, No. 1, pp. 182–191. DOI: 10.1016/j.expthermflusci.2007.03.004
[18] Senter J., Solliec C. (2007). Flow field analysis of a turbulent slot air jet impinging on a moving flat surface, *International Journal of Heat and Fluid Flow*, Vol. 28, No. 4, pp. 708–719. DOI: 10.1016/j.ijheatfluidflow.2006.08.002
[19] Ozmen Y. (2011). Confined impinging twin air jets at high Reynolds numbers, *Experimental Thermal and Fluid Science*, Vol. 35, No. 2, pp. 355–363. DOI: 10.1016/j.expthermflusci.2010.10.006
[20] Zuckerman N., Lior N. (2006). Jet impingement heat transfer: physics, correlations, and numerical modeling, *Advances in Heat Transfer*, Vol. 39, pp. 565–631. DOI: 10.1016/S0065-2717(06)39006-5
[21] Katti V., Prabhu S.V. (2008) Heat transfer enhancement on a flat surface with axisymmetric detached ribs by normal impingement of circular air jet, *International Journal of Heat and Fluid Flow*, Vol. 29, No. 5, pp. 1279–1294. DOI: 10.1016/j.ijheatfluidflow.2008.05.003
[22] Gau C., Lee C.C. (1992). Impingement cooling flow structure and heat transfer along rib-roughened walls, *International Journal of Heat and Mass Transfer*, Vol. 35, No. 11, pp. 3009–3020. DOI: 10.1016/0017-9310(92)90320-R
[23] Gau C., Lee I.C. (2000). Flow and impingement cooling heat transfer along triangular rib-roughened walls, *International Journal of Heat and Mass Transfer*, Vol. 43, No. 24, pp. 4405–4418. DOI: 10.1016/S0017-9310(00)00064-8
[24] Tan L., Zhang J. Z., Xu H.S. (2014). Jet impingement on a rib-roughened wall inside semi-confined channel, *International Journal of Thermal Sciences*, Vol. 86, pp. 210–218. DOI: 10.1016/j.ijthermalsci.2014.06.037
[25] Baydar E., Ozmen Y. (2005). An experimental and numerical investigation on a confined impinging air jet at high Reynolds numbers, *Applied Thermal Engineering*, Vol. 25, No. 2, pp. 409–421. DOI: 10.1016/j.applthermaleng.2004.05.016
[26] Abdel-Fattah A. (2007). Numerical and experimental study of turbulent impinging twin-jet flow, *Experimental Thermal and Fluid Science*, Vol. 31, No. 8, pp. 1061–1072. DOI: 10.1016/j.expthermflusci.2006.11.006
[27] Sagot B., Antonini G., Christgen A., Buron F. (2008). Jet impingement heat transfer on a flat plate at a constant wall temperature, *International Journal of Thermal Sciences*, Vol. 47, No. 12, pp. 1610–1619. DOI: 10.1016/j.ijthermalsci.2007.10.020
[28] Öztekin E., Aydin O., Avc M. (2012). Hydrodynamics of a turbulent slot jet flow impinging on a concave surface, *International Communication in Heat and Mass Transfer*, Vol. 39, No. 10, pp. 1631–1638. DOI: 10.1016/j.icheatmasstransfer.2012.10.015
[29] Caggese O., Gnaegi G., Hannema G., Terzis A., Ott P. (2013). Experimental and numerical investigation of a fully confined impingement round jet, *International Journal of Heat and Mass Transfer*, Vol. 65, pp. 873–882. DOI: 10.1016/j.ijheatmasstransfer.2013.06.043
[30] Dutta R., Dewan A., Srinivasan B. (2013). Comparison of various integration to wall (ITW) RANS models for predicting turbulent slot jet impingement heat transfer, *International Journal of Heat and Mass Transfer*, Vol. 65, pp. 750–764. DOI: 10.1016/j.ijheatmasstransfer.2013.06.056
[31] Behnia M., Parneix S., Durbin P.A. (1998). Prediction of heat transfer in an axisymmetric turbulent jet impinging on a flat plate, *International Journal of Heat and Mass Transfer*, Vol. 41, No. 12, pp. 1845–1855. DOI: 10.1016/S0017-9310(97)00254-8
[32] Craft T.J., Graham L.J.W., Launder B.E. (1993). Impinging jet studies for turbulence model assessment-II. An examination of the performance of four turbulence models, *International Journal of Heat and Mass Transfer*, Vol. 36, No. 10, pp. 2685–2697. DOI: 10.1016/S0017-9310(05)80205-4
[33] Hofmann H.M., Kaiser R., Kind M., Martin H. (2007). Calculations of steady and pulsating impinging jets—an assessment of 13 widely used turbulence models, *Numerical Heat Transfer, Part B: Fundamentals*, Vol. 51, No. 6, pp. 565–583, 2007. DOI: 10.1080/10407790701227328
[34] Al-Sanea S. (1992). A numerical study of the flow and heattransfer characteristics of an impinging laminar slot-jet including crossflow effects, *International Journal of Heat and Mass Transfer*, Vol. 35, No. 10, pp. 2501–2513. DOI: 10.1016/0017-9310(92)90092-7
[35] Sharif M.A.R., Banerjee A. (2009). Numerical analysis of heat transfer due to confined slot-jet impingement on a moving plate, *Applied Thermal Engineering*, Vol. 29, No. 2, pp. 532–540. DOI: 10.1016/j.applthermaleng.2008.03.011
[36] Arquis E., Rady M.A., Nada S.A. (2007). A numerical investigation and parametric study of cooling an array of multiple protruding heat sources by a laminar slot air jet, *International Journal of Heat and Fluid Flow*, Vol. 28, No. 4, pp. 787–805. DOI: 10.1016/j.ijheatfluidflow.2006.09.004
[37] Heyerichs K., Pollard A. (1996). Heat transfer in separated and impinging turbulent flows, *International Journal of Heat and Mass Transfer*, Vol. 39, No. 12, pp. 2385–2400. DOI: 10.1016/0017-9310(95)00347-9
[38] Wang S.J., Mujumdar A.S. (2005). A comparative study of five low Reynolds number *k-ε* models for impingement heat transfer, *Applied Thermal Engineering*, Vol. 25, No. 1, pp. 31–44. DOI: 10.1016/j.applthermaleng.2004.06.001
[39] Behnia M., Parneix S., Shabany Y., Durbin P.A. (1999). Numerical study of turbulent heat transfer in confined and unconfined impinging jets, *International Journal of Heat and Fluid Flow*, Vol. 20, No. 1, pp. 1–9. DOI: 10.1016/S0142-727X(98)10040-1
[40] Yang Y.-T., Tsai S.-Y. (2007). Numerical study of transient conjugate heat transfer of a turbulent impinging jet, *International Journal of Heat and Mass Transfer*, Vol. 50, No. 5 pp. 799–807. DOI: 10.1016/j.ijheatmasstransfer.2006.08.022
[41] Draksler M., Končar B. (2011). Analysis of heat transfer and flow characteristics in turbulent impinging jet," *Nuclear Engineering and Design*, Vol. 241, No. 4, pp. 1248–1254. DOI: 10.1016/j.nucengdes.2010.03.037
[42] Yang Y.T., Wei T.C., Wang Y.H. (2011). Numerical study of turbulent slot jet impingement cooling on a

semi-circular concave surface, *International Journal of Heat and Mass Transfer*, Vol. 54, No. 1, pp. 482–489. DOI: 10.1016/j.ijheatmasstransfer.2010.09.021

[43] Xu P., Yu B., Qiu S., Poh H.J., Mujumdar A.S. (2010). Turbulent impinging jet heat transfer enhancement due to intermittent pulsation, *International Journal of Thermal Sciences*, Vol. 49, No. 7, pp. 1247–1252. DOI: 10.1016/j.ijthermalsci.2010.01.020

[44] Pakhomov M.A., Terekhov V.I. (2005). Numerical study of fluid flow and heat transfer characteristics in an intermittent turbulent impinging round jet, *International Journal of Thermal Sciences*, Vol. 87, pp. 85–93. DOI: 10.1016/j.ijthermalsci.2014.08.007

[45] Dutta R., Dewan A., Srinivasan B. (2015). CFD study of slot jet impingement heat transfer with nanofluids, *Proceedings of the Institution of Mechanical Engineers, Part C: Journal of Mechanical Engineering Science*, Vol. 230, No. 2, pp. 206-220. DOI: 10.1177/0954406215583521

[46] Cziesla T., Biswas G., Chattopadhyay H., Mitra N.K.K. (2001). Large-eddy simulation of flow and heat transfer in an impinging slot jet, *International Journal of Heat and Fluid Flow*, Vol. 22, No. 5, pp. 500–508. DOI: 10.1016/S0142-727X(01)00105-9

[47] Uddin N., Neumann S.O., Weigand B. (2013). LES simulations of an impinging jet: on the origin of the second peak in the Nusselt number distribution, *International Journal of Heat and Mass Transfer*, Vol. 57, No. 1, pp. 356–368. DOI: 10.1016/j.ijheatmasstransfer.2012.10.052

[48] Dutta R., Srinivasan B., Dewan A. (2013). LES of a turbulent slot impinging jet to predict fluid flow and heat transfer, *Numerical Heat Transfer, Part A: Applications*, Vol. 64, No. 10, pp. 759–776. DOI: 10.1080/10407782.2013.798577

[49] Dairay T., Fortuné V., Lamballais E., Brizzi L.E. (2014). LES of a turbulent jet impinging on a heated wall using high-order numerical schemes, *International Journal of Heat and Fluid Flow*, Vol. 50, pp. 177–187. DOI: 10.1016/j.ijheatfluidflow.2014.08.001

[50] Dutta R., Dewan A., Srinivasan B. (2016). Large eddy simulation of turbulent slot jet impingement heat transfer at small nozzle-to-plate spacing, *Heat Transfer Engineering*, Vol. 37, No. 15, pp. 1242-1251. DOI: 10.1080/01457632.2015.1119592

[51] Beaubert F., Viazzo S. (2002). Large eddy simulation of a plane impinging jet, *CRAS Mecanique*, Vol. 330, No. 12, pp. 803–810. DOI: 10.1016/S1631-0721(02)01537-1

[52] Chattopadhyay H., Saha S.K. (2003). Turbulent flow and heat transfer from a slot jet impinging on a moving plate, *International Journal of Heat and Fluid Flow*, Vol. 24, No. 5, pp. 685–697. DOI: 10.1016/S0142-727X(03)00062-6

[53] Icardi M., Gavi E., Marchisio D.L., Olsen M.G., Fox R.O., Lakehal D. (2011). Validation of LES predictions for turbulent flow in a confined impinging jets reactor, *Applied Mathematical Modelling*, Vol. 35, No. 4, pp. 1591–1602. DOI: 10.1016/j.apm.2010.09.035

[54] Gao S., Voke P.R. (1995). Large-eddy simulation of turbulent heat transport in enclosed impinging jets, *International Journal of Heat and Fluid Flow*, Vol. 16, No. 5, pp. 349–356. DOI: 10.1016/0142-727X(95)00050-Z

[55] Voke P.R., Gao S. (1998). Numerical study of heat transfer from an impinging jet," *International Journal of Heat and Mass Transfer*, Vol. 41, No. 4-5, pp. 671–680. DOI: 10.1016/S0017-9310(97)00243-3

[56] Olsson M., Fuchs L. (1998). Large eddy simulations of a forced semiconfined circular impinging jet, *Physics of Fluids*, Vol. 10, No. 2, pp. 476-486. DOI: 10.1063/1.869535

[57] Tsubokura M., Kobayashi T., Taniguchi N., Jones W.P. (2003). A numerical study on the eddy structures of impinging jets excited at the inlet, *International Journal of Heat and Fluid Flow*, Vol. 24, No. 4, pp. 500–511. DOI: 10.1016/S0142-727X(03)00044-4

[58] Beaubert F., Viazzo S. (2003). Large eddy simulations of plane turbulent impinging jets at moderate Reynolds numbers, *International Journal of Heat and Fluid Flow*, Vol. 24, No. 4, pp. 512–519. DOI: 10.1016/S0142-727X(03)00045-6

[59] Yu M., Chen L., Jin H., Fan J. (2005). Large eddy simulation of coherent structure of impinging jet, *Journal of Thermal Science*, Vol. 14, No. 2, pp. 150–155. DOI: 10.1007/s11630-005-0026-y

[60] Hadžiabdić M., Hanjalić K. (2008). Vortical structures and heat transfer in a round impinging jet, *Journal of Fluid Mechanics*, Vol. 596, pp. 221–260. DOI: 10.1017/S002211200700955X

[61] Rhea S., Bini M., Fairweather M., Jones W.P. (2009). RANS modelling and LES of a single-phase, impinging plane jet, *Computers and Chemical Engineering*, Vol. 33, No. 8, pp. 1344–1353. DOI: 10.1016/j.compchemeng.2009.01.020

[62] Uddin N., Neumann S.O., Weigand B., Younis B.A. (2009). Large-Eddy Simulations and Heat-Flux Modeling in a Turbulent Impinging Jet, *Numerical Heat Transfer, Part A: Applications*, Vol. 55, No. 10, pp. 906–930. DOI: 10.1080/10407780902959324

[63] Lodato G., Vervisch L., Domingo P. (2009). A compressible wall-adapting similarity mixed model for large-eddy simulation of the impinging round jet, *Physics of Fluids*, Vol. 21, No. 3, pp. 1-21. DOI: 10.1063/1.3068761

[64] Chung Y.M.M., Luo K.H.H., Sandham N.D.D. (2002). Numerical study of momentum and heat transfer in unsteady impinging jets, *International Journal of Heat and Fluid Flow*, Vol. 23, No. 5, pp. 592–600. DOI: 10.1016/S0142-727X(02)00155-8

[65] Hattori H., Nagano Y. (2004). Direct numerical simulation of turbulent heat transfer in plane impinging jet, *International Journal of Heat and Fluid Flow*, Vol. 25, No. 5, pp. 749–758, 2004. DOI: 10.1016/j.ijheatfluidflow.2004.05.004

[66] Jaramillo J.E., Trias F.X., Gorobets A., Pérez-Segarra C.D., Oliva A. (2012). DNS and RANS modelling of a turbulent plane impinging jet, *International Journal of Heat and Mass Transfer*, Vol. 55, No. 4, pp. 789–801. DOI: 10.1016/j.ijheatmasstransfer.2011.10.031

[67] Kubacki S., Dick E. (2010). Simulation of plane impinging jets with $k$–$\omega$ based hybrid RANS/LES models, International Journal of Heat and Fluid Flow, Vol. 31, No. 5, pp. 862–878. DOI: 10.1016/j.ijheatfluidflow.2010.04.011

[68] Kubacki S., Dick E. (2011). Hybrid RANS/LES of flow and heat transfer in round impinging jets, *International Journal of Heat and Fluid Flow*, Vol. 32, No. 3, pp. 631–651. DOI: 10.1016/j.ijheatfluidflow.2011.03.002

[69] Kubacki S., Rokicki J., Dick E. (2013). Hybrid RANS/LES computations of plane impinging jets with DES and PANS models, *International Journal of Heat and Fluid Flow*, Vol. 44,pp. 596–609. DOI: 10.1016/j.ijheatfluidflow.2013.08.014

[70] Taghinia J., Rahman M.M., Siikonen T. (2014). Numerical investigation of twin-jet impingement with hybrid-type turbulence modeling, *Applied Thermal Engineering*, Vol. 73, No. 1, pp. 650–659. DOI: 10.1016/j.applthermaleng.2014.08.022

[71] Jambunathan K., Lai E., Moss M.A., Button B.L. (1992). A review of heat transfer data for single circular jet impingement, *International Journal of Heat and Fluid Flow*, Vol. 13, No. 2, pp. 106–115. DOI: 10.1016/0142-727X(92)90017-4

[72] Viskanta R. (1993). Heat transfer to impinging isothermal gas and flame jets," *Experimental Thermal and Fluid Science*, Vol. 6, No. 2, pp. 111–134. DOI: 10.1016/0894-1777(93)90022-B

[73] Zuckerman N., Lior N. (2005). Impingement heat transfer: correlations and numerical modeling, *Journal of Heat Transfer*, Vol. 127, pp. 544-552. DOI: 10.1115/1.1861921

[74] Shukla A.K., Dewan A. (2016). Computational study on effects of rib height and thickness on heat transfer enhancement in a rib roughened square channel, S*ādhanā - Academy Proc. In Engineering Science*, Vol. 41, No. 6, pp. 667–678. DOI: 10.1007/S12046-016-0501-Z

[75] Kaliakatsos D., Cucumo M., Ferraro V., Mele M., Galloro A., Accorinti F. (2016). CFD analysis of a pipe equipped with twisted tape, *International Journal of Heat and Technology*, Vol. 34, No. 2, pp. 172–180. DOI: 10.18280/ijht.340203.

[76] Shukla A.K., Dewan A. (2015). Computational study of heat transfer enhancement through broken and continuous attached ribs in a square channel, *Proceedings of the 23rd National Heat and Mass Transfer Conference and 1st International ISHMT-ASTFE Heat and Mass Transfer Conference IHMTC2015*, Thiruvananthapuram, India, pp. 1–8.

[77] Huang Y., Chen L.J., Li M.J., Zhang B., Zhang L.N. (2016). Comparative study on the performance of flat tube type and wasp-waisted tube type radiators, *International Journal of Heat and Technology*, Vol. 34, No. 4, pp. 647-652. DOI: 10.18280/ijht.340414

[78] Shukla A.K., Dewan A., Srinivasan B. (2016). Computational study of turbulent slot jet impingement on a ribbed surface, *Proceedings of the 6th International and 43rd National Conference on Fluid Mechanics and Fluid Power*, MNNIT Allahabad, India.

[79] Lorenzini G., Saro O. (2013). Thermal fluid dynamic modelling of a water droplet evaporating in air, *International Journal of Heat and Mass Transfer*, Vol. 62, pp. 323-335. DOI: 10.1016/j.ijheatmasstransfer.2013.02.062

[80] Wrachien D.D., Lorenzini G., Medici M. (2013). Sprinkler irrigation systems: state-of-the-art of kinematic analysis and quantum mechanics applied to water jets, *Irrigation and drainage*, Vol. 62, No. 4, pp. 407-413. DOI: 10.1002/ird.1759

[81] Spalart P.R. (2000). Strategies for turbulence modeling and simulation, *Int. J. of Heat and Fluid Flow*, Vol. 21, No. 3, pp. 252-263. DOI: 10.1016/S0142-727X(00)00007-2

[82] Liu L.L., Sun Z.C., Wan C.L., Wu J.M. (2015). Jet Flow Field Calculation & Mechanism Analysis on Hot-Air Drying Oven Based on RNG k-ε model, *International Journal of Heat and Technology*, Vol. 33, No. 1, pp. 77–82. DOI: 10.18280/ijht.330111

[83] Dewan A. (2011). *Tackling Turbulent Flows in Engineering*, Springer Berlin Heidelberg. DOI: 10.1007/978-3-642-14767-8

[84] Wilcox D.C. (2006). *Turbulence Modeling for CFD*, 3rd Edition, DCW Industries, USA.

[85] Girimaji S.S. (2006b). Partially-averaged Navier-Stokes Model for turbulence: a Reynolds-averaged Navier-Stokes to direct numerical simulation bridging method, *Journal of Applied Mechanics*, Vol. 73, No. 3, pp. 413-421. DOI: 10.1115/1.2151207

## NOMENCLATURE

| | |
|---|---|
| *B (W)* | slot width |
| *c* | rib clearance |
| *c/e* | non-dimensional rib clearance |
| *D* | nozzle exit diameter |
| *e* | rib height |
| *H* | height between nozzle to plate |
| *H/B or H/D* | normalized nozzle to plate spacing |
| *h* | heat transfer coefficient *(W/m$^2$-K)* |
| $k_f$ | thermal conductivity *(W/m-K)* |
| *Nu* | Nusselt number (*hB/k*) |
| *P* | mean pressure |
| *p/e* | normalized rib pitch |
| *Re* | Reynolds number ($\rho UB/\mu$) |
| *T* | mean temperature |
| *U* | mean velocity |
| *x,y,z* | coordinate directions |

### Greek symbols

| | |
|---|---|
| $\alpha$ | thermal diffusivity, $m^2/s$ |
| $\mu$ | dynamic viscosity, *kg./m.s* |

### Subscripts

| | |
|---|---|
| *f* | fluid |
| *t* | turbulent |